JACS Au
AN OPEN ACCESS JOURNAL OF THE AMERICAN CHEMICAL SOCIETY



pubs.acs.org/jacsau
Article

# Functional Upcycling of Polyurethane Thermosets into Value-Added Thermoplastics via Small-Molecule Carbamate-Assisted Decross-Linking Extrusion

Jared A. Nettles, Saleh Alfarhan, Cameron A. Pascoe, Clarissa Westover, Margaret D. Madsen, Jose I. Sintas, Aadhi Subbiah, Timothy E. Long,* and Kailong Jin*

Cite This: JACS Au 2024, 4, 3058−3069
Read Online

ACCESS | Metrics & More | Article Recommendations | Supporting Information

**ABSTRACT:** The cross-linked structures of most commodity polyurethanes (PUs) hinder their recycling by common mechanical/chemical approaches. Catalyzed dynamic carbamate exchange emerges as a promising PU recycling strategy, which converts traditional static PU thermosets into reprocessable covalent adaptable networks (CANs). However, this approach has been limited to thermoset-to-thermoset reprocessing of PU CANs, accompanied by their well-preserved network structures and extremely high viscosities, which pose challenges to processing and certain applications. This study reports a catalytic decross-linking extrusion process aided by small-molecule carbamates, which can upcycle PU thermosets into easily processable and functional PU thermoplastics in a solvent-free and high-throughput manner. Key to this process is the employment of small-molecule carbamates as decross-linkers to simultaneously deconstruct cross-linked PUs and functionalize the decross-linked PU chains, through catalyzed carbamate exchange reactions in a twin-screw extruder. This strategy applies to both aromatic and aliphatic cross-linked PU films and foams, and the amount of small-molecule carbamates required to decross-link PU networks is determined through thermal, chemical, and structural analyses of the resulting extrudates. This approach is generalizable to small-molecule carbamates with various steric/electronic structures and chemical functionalities including methacrylate, anthracene, and stilbene groups. The chain-end functionalization is confirmed by analyzing the purified decross-linked extrudates after dialysis. This thermoset-to-thermoplastic extrusion process represents a powerful approach for upcycling postconsumer PU thermosets into a library of thermoplastic PUs with controlled molecular weights and chain-end functionalities for diverse applications, including adhesives, photoresins, and stimuli-responsive materials, as demonstrated herein. In the future, this strategy could be extended to upcycle many other step-growth networks capable of undergoing catalytic bond exchange reactions, such as cross-linked polyureas and polyesters, contributing to plastic waste management in general.

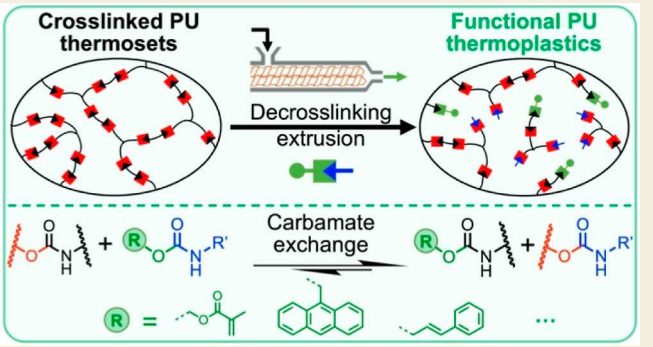


**KEYWORDS:** *cross-linked polyurethane, polyurethane depolymerization, reactive extrusion, carbamate bond exchange, covalent adaptable networks, plastic recycling, sustainability*



## 1. INTRODUCTION

Polyurethanes (PUs) are the sixth-largest manufactured consumer plastics, with a global market volume of ∼56 billion pounds (∼$87 billion market value) in 2023 and it expected to reach ∼69 billion pounds (∼$120 billion market value) by 2030.[1,2] Due to their tunable material properties, PUs are widely used in applications ranging from CASE industries—coatings, adhesives, sealants, and elastomers—to PU foams (PUFs) for comfort and construction, where PUs are commonly synthesized as cross-linked thermosets.[3−6] Their permanent network structures prohibit recycling via conventional melt processing techniques used to recycle thermoplastics, leading to a low end-of-life PU recycling rate of only 5.5%.[7,8] A current PU recycling approach is the mechanical repurposing of cross-linked PUs toward low-end applications, e.g., PUFs are ground and combined with binders to produce carpet underlayers.[7,9] Another approach is chemical recycling such as glycolysis, which typically employs solvents, heat, and long reaction times to break carbamate linkages (i.e., urethane bonds) and depolymerize PUs into oligomers, followed by energy-intensive multistep separation processes to recover PU

Received: May 3, 2024
Revised: June 22, 2024
Accepted: June 28, 2024
Published: July 12, 2024

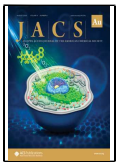

**Scheme 1. Upcycling of Crosslinked PU Thermosets into Functional PU Thermoplastics via Small-Molecule Carbamate-Assisted Decross-Linking Extrusion, Where Small-Molecule Carbamates Undergo Catalyzed Carbamate Exchange Reactions with Crosslinked PU in a Twin-Screw Extruder, Producing Decross-Linked (Linear/Branched) and Functional PU Chains Toward Value-Added Applications**

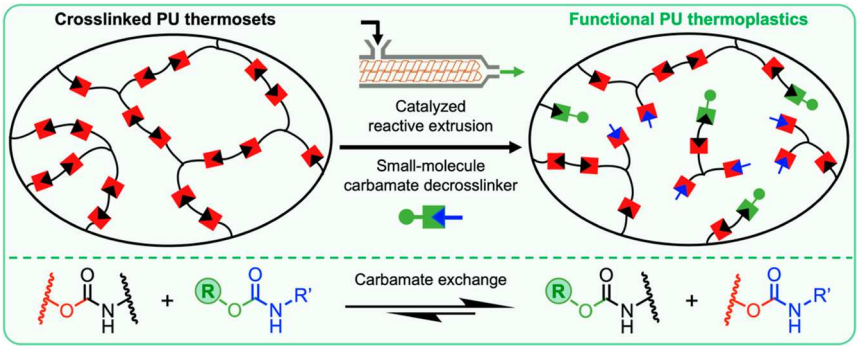


precursors (i.e., polyols).[7,9−14] Both of these two common methods have their own limitations,[15,16] which motivate the development of more circular and efficient PU recycling strategies.

Recent studies have reported potential, alternative PU recycling strategies that convert traditional static PU networks into thermally reprocessable, dynamic covalent adaptable networks (CANs[17]) by incorporating Lewis acid catalysts such as dibutyltin dilaurate (DBTDL), either during the synthesis of new PUs or before reprocessing postconsumer PUs.[18−27] The incorporated catalysts trigger dynamic carbamate exchange reactions at elevated temperatures (typically 180−220 °C), enabling these PU CANs to reshape under stress like thermoplastics during conventional melt-state processing such as compression molding and twin-screw extrusion,[18−22] similar to many other CANs and vitrimers.[28−41] In contrast, at lower service temperatures, these PU CANs maintain network structures and thermomechanical robustness like traditional PU thermosets.[17−22] With this approach, Dichtel and co-workers reprocessed waste cross-linked PUs (e.g., PUFs) into recycled PU films/filaments with equivalent network structures and properties, through a bulk (i.e., solvent-free), continuous twin-screw extrusion process.[21] More recently, they further demonstrated a circular foam-to-foam recycling process, which simultaneously combines twin-screw extrusion with foaming to convert originally cross-linked PUFs into next-generation cross-linked PUFs with comparable porous microstructures and compression properties.[22]

Despite the advantages of this dynamic carbamate exchange-enabled recycling approach, including circularity and high energy/atom efficiency, previous studies have been limited to thermoset-to-thermoset reprocessing of PU CANs.[18−27] The percolated network structures and associated high viscosities of these PU CANs pose challenges to their processing and engineering for certain applications that require low-viscosity liquid precursors, such as coatings, adhesives, and sealants.[31,32,42] Of greater utility would be a scalable recycling/upcycling strategy that can convert postconsumer cross-linked PUs into a library of materials/products with similar or even higher values for diverse applications. For example, it would be attractive if one can upcycle waste cross-linked PUs into readily processable/soluble and functionalized PUs toward high-end specialty applications, such as photocurable liquid PU resins that can be used for conformal coatings and vat photopolymerization-based additive manufacturing (i.e., 3D printing).[39,42−47]

Herein, we report a catalytic decross-linking extrusion process aided by small-molecule carbamate decross-linkers, which recycles/upcycles cross-linked PU thermosets into a library of processable and functional thermoplastic PUs in a solvent-free and high-throughput manner. In this one-step process, small-molecule carbamates undergo fast, catalyzed carbamate exchange reactions with cross-linked PU feedstocks (both films and foams) during catalytic reactive extrusion (Scheme 1), serving as end-capping reagents to rapidly decrease cross-link density and ultimately deconstruct PU networks into low-viscosity, solution-processable decross-linked PU chains. Importantly, simultaneous functional design of these small-molecule carbamate decross-linkers enables facile installation of desired chain-end functionalities onto the resulting decross-linked PUs for target applications, such as methacrylate-functionalized PU chains for subsequent photocuring. The process demonstrated herein represents an alternative strategy capable of transforming waste PU thermosets at scale into value-added thermoplastic PU feedstocks, which can be directly utilized without further purification for diverse applications including adhesives, photoresins for coatings/3D printing, and stimuli-responsive materials. This methodology is particularly attractive for sustainable PU recycling/upcycling, considering its advantages including relatively mild reaction conditions, fast reaction rates, compatibility with the well-established polymer processing equipment, and highly modular structure−property−function relationships of the recycled/upcycled PU products.

## 2. EXPERIMENTAL METHODS

### 2.1. General Procedure for the Synthesis of Small-Molecule Carbamate Decross-Linkers

All the small-molecule carbamates listed in Table 1 (except for **M4**) were synthesized in a similar manner by reacting monofunctional isocyanates with monofunctional alcohols (10 mol % excess). In a typical synthesis of the model small-molecule carbamate **M1** in Table 1, stearyl alcohol (12.5 g, 46.2 mmol) was first dissolved in anhydrous tetrahydrofuran (THF; 100 mL) in a round-bottom flask equipped with a magnetic stir bar, rubber septa, nitrogen inlet, and nitrogen outlet, which was held at 0 °C in an ice bath. Phenyl isocyanate (5.0 g, 42.0 mmol) and DBTDL (0.133 g, 0.21 mmol, 0.5 mol % of the total amount of isocyanate groups) were then added to the flask, and the resulting mixture was allowed to react for 2 h before precipitation into methanol (1 L). The precipitated products were collected by filtration


https://doi.org/10.1021/jacsau.4c00403
JACS Au 2024, 4, 3058−3069

**Table 1. Small-Molecule Carbamates Synthesized and Used as Decross-Linkers in This Study, Highlighting Their Molecular Structures, Melting Points ($T_m$) Measured by DSC, and Onset Temperatures of Volatilization/Decomposition ($T_{v/D}$) Measured by TGA. (Melting of F2 is Not Detected during DSC Heating Scan up to 120 °C.)**

| Small-molecule carbamates | Molecular structures | $T_m$ values by DSC (± 1 °C) | $T_{v/d}$ values by TGA (± 3 °C) |
|---|---|---|---|
| M1 (Stearyl N-phenyl carbamate) | 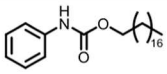 | 78 | 178 |
| M2 (Stearyl N-cyclohexyl carbamate) | 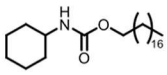 | 70 | 180 |
| M3 (Benzyl N-cyclohexyl carbamate) | 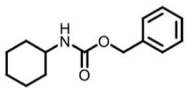 | 92 | 152 |
| M4 (Stearyl N-butyl carbamate) | 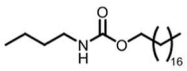 | 68 | 141 |
| F1 (HEMA N-phenyl carbamate) | 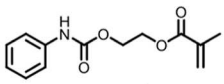 | 60 | 211 |
| F2 (Anthracenemethanol N-phenyl carbamate) | 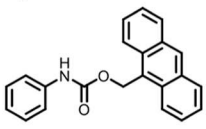 | - | 189 |
| F3 (Cinnamyl N-phenyl carbamate) | 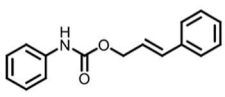 | 90 | 173 |

and rinsed with 500 mL methanol, followed by vacuum drying at 40 °C for 6 h to yield white crystalline solids at room temperature. Supporting Information provides the detailed synthesis procedures for all the small-molecule carbamates in Table 1, together with their characterizations by Fourier-transform infrared (FTIR) spectroscopy, nuclear magnetic resonance (NMR) spectrometry, differential scanning calorimetry (DSC), and thermogravimetric analysis (TGA) (Schemes S1−S7 and Figures S1−S7).

### 2.2. General Procedure for the Deconstruction of Cross-Linked PUs via Small-Molecule Carbamate-Assisted Decross-Linking Extrusion

Cross-linked PU films and foams were decross-linked by small-molecule carbamates through bulk-catalyzed carbamate exchange reactions in a twin-screw extruder. In a representative model PU film decross-linking experiment using **M1** (Table 1), dry model cross-linked PU films (3.500 g, containing 8.2 mmol of carbamate linkages) were ground and fed into an Xplore microcompounder (5 mL capacity, recirculated twin-screw extrusion design) held at 165 ± 10 °C, together with **M1** (1.069 g, containing 2.74 mmol of carbamate linkages; 25.0 mol % of the total carbamate linkages in both small-molecule carbamate decross-linkers and model cross-linked PU films) and DBTDL catalysts (0.277 g, 0.44 mmol, 4.0 mol % of the total carbamate linkages in the feed mixture). The feed materials were mixed at 150 rpm for 8 min under a nitrogen atmosphere before extrusion, affording homogeneous, transparent, and low-viscosity liquid extrudates light tan in color. The resulting extrudates were either used/characterized as extruded or after dialysis purification using cellulose tubing with a 3 kg $mol^{-1}$ molecular weight cutoff. Supporting Information provides the detailed procedures for the syntheses of model cross-linked PU films/foams and the decross-linking extrusion experiments using all the small-molecule carbamates listed in Table 1, together with their FTIR, NMR, DSC, TGA, and rheological characterizations (Schemes S8−S17 and Figures S8−S24). Supporting Information also describes preliminary decross-linking extrusion tests under various processing conditions such as extrusion temperature, reaction time, catalyst concentration, and small-molecule carbamate decross-linker loading.

## 3. RESULTS AND DISCUSSION

### 3.1. Small-Molecule Carbamate Decross-Linker Design and Synthesis

Table 1 compiles the small-molecule carbamates synthesized and used as decross-linkers in this study, which are stearyl *N*-phenyl carbamate (noted as **M1**), stearyl *N*-cyclohexyl carbamate (**M2**), benzyl *N*-cyclohexyl carbamate (**M3**), stearyl *N*-butyl carbamate (**M4**), hydroxyethyl methacrylate *N*-phenyl carbamate (**F1**), anthracenemethanol *N*-phenyl carbamate (**F2**), and cinnamyl *N*-phenyl carbamate (**F3**). **M1** serves as a model small-molecule carbamate decross-linker for establishing the catalytic decross-linking extrusion process and studying key reaction parameters. **M2**, **M3**, and **M4** are selected to study how small-molecule carbamates' steric and electronic structures affect the overall PU decross-linking extrusion process, while **F1**, **F2**, and **F3** are used to simultaneously incorporate chain-end functionalities including methacrylate, anthracene, and stilbene groups.

Specifically, all the small-molecule carbamates listed in Table 1 (except for **M4**) were synthesized by reacting monofunctional isocyanates with monofunctional alcohols (10 mol % excess), followed by precipitation and drying (see Supporting Information for synthesis and purification details). Notably, **M4** was synthesized using carbonyl diimidazole, demonstrating an alternative isocyanate-free route to these small-molecule carbamate decross-linkers.[48,49] $^{1}H$ and $^{13}C$ NMR as well as FTIR analyses (Figures S1−S7) of these synthesized small-molecule carbamates confirm their expected chemical structures, as shown in Table 1. All these small-molecule carbamates are solids at room temperature and report melting points ($T_m$) between 60 and 92 °C (except **F2**), as measured by DSC (Figures S1−S7). In addition, they report onset temperatures of volatilization/decomposition (noted as $T_{v/d}$) between 141 and 211 °C, as measured by TGA (Figures S1−S7).

### 3.2. Model PU Network Deconstruction via Small-Molecule Carbamate-Assisted Extrusion

A catalytic PU decross-linking process was achieved by reactive extrusion of cross-linked PU with small-molecule carbamate decross-linkers to induce simultaneous network deconstruction and chain-end functionalization during melt-state processing in a solvent-free manner. The initial model cross-linked PU films were prepared by step-growth polymerization of a stoichiometric alcohol/isocyanate (−OH/−NCO) mixture of polyethylene glycol-based triol and 2,4-toluene diisocyanate (toluene diisocyanate (TDI)) at room temperature under a nitrogen atmosphere.[50] Cross-linking of these model PU films is confirmed by their insolubility and swelling behavior in dichloromethane. Quantitative swelling tests of these model cross-linked PU films report a relatively high gel fraction of ∼95 wt %, in agreement with the nearly full consumption of −OH and −NCO groups after polymerization, as measured by FTIR (Figure S8). Consistently, rheological frequency sweep of these model PU films at room temperature reveals an elastic shear modulus ($G'$) plateau at low frequency (Figure S8),


https://doi.org/10.1021/jacsau.4c00403
JACS Au 2024, 4, 3058−3069

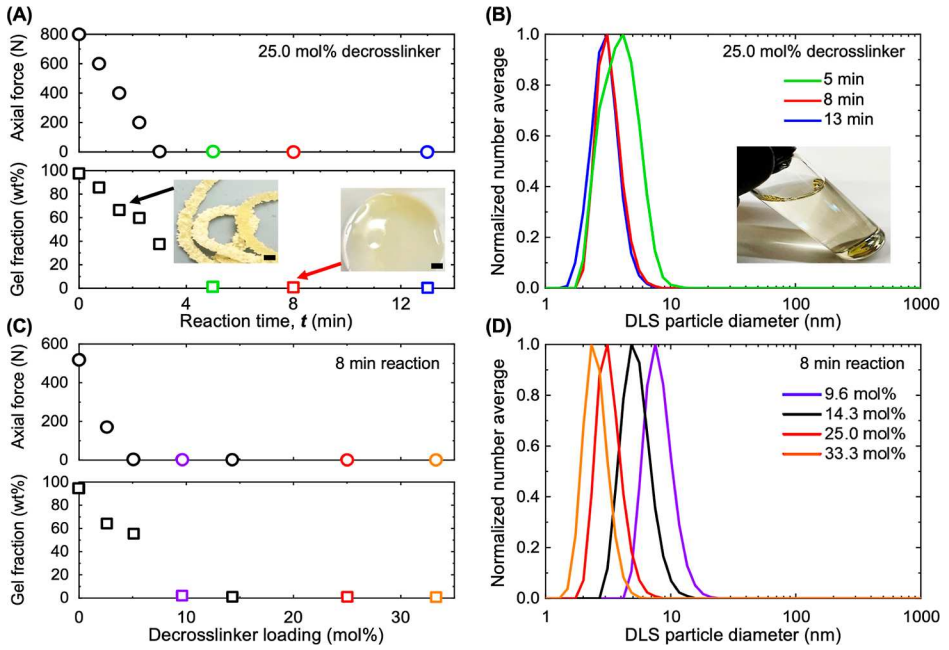


**Figure 1.** Decross-linking extrusion of the model cross-linked PU film with small-molecule carbamate decross-linker **M1**: (A) extruder's axial force and the resulting extrudate's gel fraction as functions of reaction time $t$ at 25.0 mol % **M1** loading; (B) dynamic light scattering (DLS) spectra of the decross-linked extrudates obtained at $t$ = 5, 8, and 13 min in (A); (C) extruder's axial force and the resulting extrudate's gel fraction as functions of **M1** loading at $t$ = 8 min; and (D) DLS spectra of the decross-linked extrudates obtained with 9.6, 14.3, 25.0, and 33.3 mol % **M1** in (C). The scale bars in the inset photographs in (A) are 5 mm. The experimental errors in (A,C) are standard deviations from three measurements, which are smaller than the symbol sizes.

characteristic of a cross-linked elastic solid.[51] In addition, these model cross-linked PU films report a glass transition temperature ($T_g$; measured by DSC) of ∼−30 °C and degradation temperature ($T_d$; measured by TGA) of ∼280 °C, respectively (Figure S8).

Catalytic PU decross-linking was carried out by feeding the dry, ground model cross-linked PU films [average particle diameter of 1.6 ± 0.4 mm, as measured by scanning electron microscopy (SEM); Figure S9], together with the target small-molecule carbamate decross-linkers and DBTDL carbamate exchange catalysts into a twin-screw extruder. The reactive extrusion temperature was held at 165 ± 10 °C throughout this study, which is below the $T_{v/d}$ values of the small-molecule carbamates in Table 1 (except for **M3** and **M4**) and DBTDL (>280 °C). It is noteworthy that all the small-molecule carbamates fed into the extruder exhibited no or negligible weight loss due to volatilization/decomposition during reactive extrusion in the tightly sealed extrusion chamber. It is also noteworthy that DBTDL can be replaced by lower-toxicity catalysts such as zirconium(IV) acetylacetonate [$Zr(acac)_4$], which have been recently demonstrated to be effective in enhancing carbamate exchange rates.[52,53] As these model cross-linked PU film granules are heated inside the twin-screw extruder, the reversible urethane dissociation and recombination enable the PU network to undergo deconstruction via catalyzed carbamate exchange reactions with the small-molecule carbamate decross-linkers.[21,22]

The fundamental principle of this small-molecule carbamate-assisted PU decross-linking process builds on the reverse of the classical Flory−Stockmayer "gelation" theory,[54,55] which predicts the minimum level of branch unit incorporation or conversion to achieve a percolated network, i.e., gelation, during step-growth polymerization.[51,56] Herein, any small-molecule carbamate decross-linker in Table 1 can be treated as a stoichiometric mixture of monofunctional alcohols and monofunctional isocyanates at full functional group conversion, while the model cross-linked PU film can be treated as a stoichiometric mixture of trifunctional alcohols (i.e., cross-linker or branch unit; functionality $f$ = 3) and difunctional isocyanates at full functional group conversion. The ratio between the added small-molecule carbamate decross-linkers and the model cross-linked PU dictates the probability of a cross-linker leading to another cross-linker by a chain ($\alpha$; also known as branching coefficient) in an equivalent polymerization mixture comprising equimolar monofunctional alcohols and isocyanates as well as stoichiometrically balanced trifunctional alcohols and difunctional isocyanates. In order for complete deconstruction of the originally cross-linked PU, i.e., no percolated network formation in the equivalent polymerization mixture, $\alpha$ must be smaller than the critical value for gelation, $\alpha_c$, where $\alpha_c = 1/(f-1) = 0.5$ in this study. Based on this simple analysis, the amount of small-molecule carbamate decross-linkers required to deconstruct the model cross-linked PU is ∼30 mol % relative to the total amount of the carbamate linkages in the entire feed mixture (see Supporting Information for full derivations).

It is noteworthy that this simple theoretical analysis is expected to overestimate the amount of small-molecule carbamate decross-linkers required to deconstruct the PU network. This is because the classical Flory−Stockmayer theory builds on simplified assumptions of equal functional group reactivities and ignores potential intramolecular reactions leading to loops that do not contribute to network formation.[51,54−56]

Our initial decross-linking extrusion experiments focused on a model system comprising 3.500 g of model cross-linked PU films (8.2 mmol of carbamate linkages), 1.069 g of model small-molecule carbamates **M1** (2.74 mmol of carbamate


https://doi.org/10.1021/jacsau.4c00403
JACS Au 2024, 4, 3058−3069

linkages; 25.0 mol % of the total number of carbamate linkages in the feed mixture, greater than the required decross-linker amount predicted above), and 0.277 g of DBTDL catalysts (4.0 mol % of the total number of carbamate linkages). Figure 1A (top) plots the evolution of the extruder's axial force, a measure of the reaction mixture's viscosity, with increasing mixing time $t$, which decreases steadily from ∼800 N at $t$ = 0 min to ∼0 N at $t \approx 3$ min. In contrast, the same mixture without the incorporation of DBTDL exhibits a nearly unchanged axial force at ∼800 N over time under the same mixing conditions, indicating that carbamate exchange catalysts are indeed required to catalyze the reactions between cross-linked PU and small-molecule carbamate decross-linkers.

Qualitatively consistent with the decreasing trend of extruder's axial force with increasing $t$, the corresponding PU extrudates obtained after catalytic extrusion appear as heterogeneous, light tan-colored solids at shorter $t$, but they transform into homogeneous, transparent, and viscous liquids light tan in color at longer $t$ (Figure 1A bottom; inset photographs). Quantitatively, Figure 1A (bottom) plots the $t$-dependent gel fraction of the resulting extrudates, which decreases from ∼95 wt % at $t$ = 0 min to ∼0 wt % at $t$ = 5 min. This indicates the complete deconstruction of cross-linked PU networks at or after $t$ = 5 min into decross-linked (linear or branched) PU chains that are completely soluble in THF (Figure 1B; inset photograph). Consistently, rheological frequency sweep of the extrudates obtained after reacting for 8 min confirms complete PU network deconstruction; i.e., their $G'$ and $G''$ moduli at 80 °C (where the hydrogen bonding between carbamate linkages is relatively weak[57,58]) exhibit liquid-like scaling at low frequency (Figure S11).[51] Notably, the FTIR spectra of the resulting decross-linked extrudates resemble those of initial feed mixtures (Figure S11), both showing characteristic peaks for urethane linkages and no evidence for new chemical bond formation. In addition, NMR analyses of the resulting extrudates in the Supporting Information confirm the complete deconstruction of cross-linked PU and the conservation of carbamate linkages after decross-linking extrusion. All these results are consistent with the PU network deconstruction mechanism/process through catalyzed carbamate exchange reactions with small-molecule carbamate decross-linkers.

Figure 1B compiles the corresponding DLS spectra for dilute THF solutions of the decross-linked PU extrudates in Figure 1A. According to Figure 1B, these extrudates' hydrodynamic diameter ($D_h$) distribution curves shift to smaller sizes and become narrower with increasing $t$. Specifically, the $D_h$ distribution at $t$ = 5 min appears relatively broad spanning from ∼2 to ∼12 nm and then becomes narrower ranging from ∼2 to ∼8 nm after reacting for 8 and 13 min. Correspondingly, the peak $D_h$ values initially decrease from ∼4 nm at $t$ = 5 min to ∼3 nm at $t$ = 8 min and then remain nearly unchanged at $t$ = 13 min. It is well established in the literature that a smaller $D_h$ value corresponds to a lower molecular weight.[51,59−62] For example, size exclusion chromatography (SEC) estimates a number average molecular weight ($M_n$) of ∼27 kg mol$^{-1}$ for the decross-linked PU extrudate obtained after reacting for 8 min (see Supporting Information for more SEC details). It is important to note that SEC characterizations might be convoluted by the complications from decross-linked PU extrudates' branched architectures and intramolecular hydrogen bonding interactions.[51,59,60] Collectively, DLS and SEC indicate that the decross-linked PU extrudate's molecular weight and its distribution (i.e., width of the $D_h$ distribution or breadth of the SEC elution peak) continue to evolve until $t \approx 8$ min, at which the catalyzed carbamate exchange reactions in this system likely have reached an equilibrium state.

Importantly, this small-molecule carbamate-assisted PU decross-linking process is highly modular. For example, while keeping other process parameters constant, i.e., catalyst loading = 4.0 mol %, $T$ = 165 ± 10 °C, and $t$ = 8 min, increasing the loading of model small-molecule carbamates **M1** from 2.6 to 9.6 mol % leads to respective decreases in the extruder's axial force from ∼170 to ∼0 N and the gel fraction of the resulting PU extrudates from ∼64 to ∼0 wt % (Figure 1C). As expected, the experimental critical loading of small-molecule carbamate decross-linkers at which cross-linked PU fully deconstructs (∼10 mol %, when the resulting extrudates' gel fraction drops to ∼0 wt %) is much lower than that predicted by our simple Flory−Stockmayer-like analysis (∼30 mol %; see discussion above and Supporting Information).

Further increasing the **M1** loading from 9.6 to 33.3 mol % leads to a consistent reduction in the resulting decross-linked PU extrudates' molecular weight, according to their DLS characterizations as shown in Figure 1D. As a result, the final material properties of these decross-linked PU extrudates, including $T_g$, rheological properties, and adhesion strength (see Figure S12 and Section 3.4.1 below), can be systematically tuned over a wide range. For example, as shown in Figure S12, the decross-linked PU extrudates' zero-shear melt viscosities at 80 °C decrease from ∼20 Pa·s at 14.3 mol % **M1** loading to ∼2 Pa s at 33.3 mol % **M1** loading, consistent with the well-established relationship between molecular weight and melt viscosity in the literature.[51,63]

### 3.3. Versatility of This Small-Molecule Carbamate-Assisted PU Decross-Linking Extrusion

Having established a model PU network deconstruction process in Section 3.2, we set out to test the versatility/generalizability of this decross-linking extrusion approach, by extending to other small-molecule carbamate decross-linkers, an aliphatic cross-linked PU, and cross-linked PUFs.

**3.3.1. Extension to Other Small-Molecule Carbamate Decross-Linkers.** We first extended our approach to decross-link the same model cross-linked PU films using other small-molecule carbamate decross-linkers listed in Table 1 while keeping the rest of the reactive extrusion conditions the same, i.e., decross-linker loading = 25.0 mol %, DBTDL loading = 4.0 mol %, $T$ = 165 ± 10 °C, and $t$ = 8 min. A notable small-molecule carbamate decross-linker is **F1**, which contains a reactive methacrylate group. When **F1** was employed as a decross-linker, we intentionally introduced an excess amount of butylated hydroxytoluene (BHT; molar ratio between BHT and methacrylate groups = 1.6:1) to completely suppress any unwanted methacrylate chain-growth homopolymerization during reactive extrusion.[64] Note that the BHT loading during decross-linking extrusion will be optimized in our future studies.

Promisingly, all the resulting PU extrudates after the decross-linking reaction appear as homogeneous and transparent liquids at extrusion temperature, exhibiting no or negligible (<1 wt %) gel fraction, regardless of the small-molecule carbamate decross-linkers tested in this study. (Note that a <1 wt % gel fraction in the resulting decross-linked PU extrudate corresponds to a depolymerization yield of >99% after decross-linking extrusion.) Consistently, rheological


https://doi.org/10.1021/jacsau.4c00403
JACS Au 2024, 4, 3058−3069

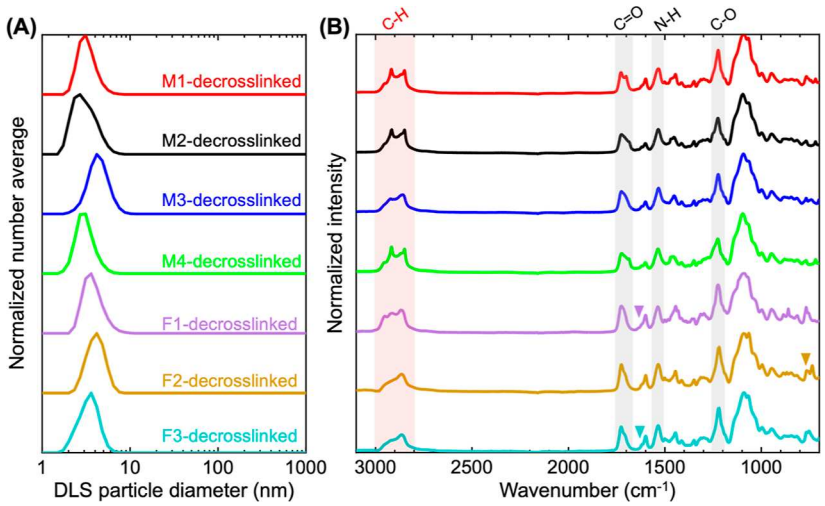


**Figure 2.** Decross-linking extrusion of the model cross-linked PU film with various small-molecule carbamate decross-linkers: (A) DLS spectra of the decross-linked extrudates obtained right after extrusion using **M1**−**4** and **F1**−**3** at $t$ = 8 min and (B) FTIR spectra of these decross-linked extrudates after dialysis. The gray- and pink-shaded regions in (B), respectively, highlight the characteristic peaks for carbamate linkages and different chain ends from **M1**−**4** and **F1**−**3**. The triangles in (B) point at the characteristic peaks for methacrylate, anthracene, and stilbene groups (see zoom-in FTIR spectra in Supporting Information for better visualization).

frequency sweep experiments on these extrudates confirm their decross-linked structures. The DLS spectra of all these as-obtained decross-linked PU extrudates in Figure 2A show $D_h$ distributions with peak values varying from ∼2.7 to ∼4.2 nm, indicating that the small-molecule carbamate's steric/chemical structure and/or functionality may slightly impact the carbamate exchange decross-linking reaction characteristics.

Figure 2B compiles the FTIR spectra of these decross-linked PU extrudates after dialysis to remove any residual small-molecule carbamates, DBTDL catalysts, and other species like BHT (see Supporting Information for dialysis details). As shown in Figure 2B, all these decross-linked PU extrudates show nearly identical characteristic peaks for carbamate linkages, e.g., ∼1720 $cm^{-1}$ for C═O stretch, ∼1535 $cm^{-1}$ for N−H bend, and ∼1220 $cm^{-1}$ for C−O stretch, respectively.[65] In addition, change in the molecular structures of carbamate decross-linkers (**M1**−**4** and **F1**−**3**) leads to notably different FTIR signals in specific wavenumber ranges, which arise from individual carbamate decross-linkers, in the resulting decross-linked extrudates. For example, the aliphatic **M4**-decross-linked extrudate exhibits much sharper $sp^3$ C−H stretch peaks in the wavenumber range between 2925 and 2845 $cm^{-1}$ than those of the highly aromatic **F2**-decross-linked extrudate (Figure 2B). Thus, the FTIR results indicate that these small-molecule carbamate decross-linkers undergo exchange reactions with the originally cross-linked PU, serving as capping reagents that modify the chain ends of decross-linked PU extrudates. Notably, a closer look at the FTIR in Figure 2B confirms the successful installation of various reactive functional groups onto decross-linked PU chains, i.e., the methacrylate group from **F1**, the anthracene group from **F2**, and the stilbene group from **F3** (Supporting Information). Consistently, NMR characterizations of all these decross-linked PU extrudates both before and after dialysis confirm the complete deconstruction of cross-linked PU by small-molecule decross-linkers through carbamate exchange reactions (Figures S13−S19). These NMR results, together with SEC results (Figure S20), provide a rough estimate of the average number of functional groups installed onto each decross-linked PU chain after decross-linking extrusion under specific conditions (See Supporting Information for more discussion).

Overall, it is demonstrated above that our catalytic PU decross-linking extrusion approach can generalize to a wide range of small-molecule carbamate decross-linkers having various steric/electronic structures and reactive/functional moieties. This paves the way for upcycling postconsumer cross-linked PU thermosets into functional PU thermoplastics for potential value-added applications (see Section 3.4).

**3.3.2. Extension to Model Aliphatic Cross-Linked PU.** We then extended our approach to decross-link a model aliphatic cross-linked PU synthesized using hexamethylene diisocyanate (HDI). Compared to those synthesized with aromatic diisocyanates like TDI, which suffer from aromaticity-induced yellowing, aliphatic PUs offer enhanced weather resistance and color stability for outdoor/coating applications.[66,67] For demonstration, model aliphatic cross-linked PU films were prepared by step-growth polymerization of a stoichiometric alcohol/isocyanate (−OH/−NCO) mixture of the same triol, as shown in Section 3.2, and HDI, in the presence a catalytic amount of DBTDL (0.5 mol % of the total −OH groups) at room temperature (see Supporting Information for details). Swelling tests of these model aliphatic PU films in dichloromethane confirm their cross-linking and report a gel fraction of ∼92 wt %. DSC reports a $T_g$ of ∼−44 °C for these aliphatic cross-linked PU films (Figure S21), ∼15 °C lower than that of the ones synthesized using aromatic TDI (Figure S8).

Promisingly, the decross-linking extrusion conditions of these aliphatic cross-linked PU films closely mirrored those of their aromatic counterparts, i.e., 25.0 mol % **M1**, DBTDL loading = 4.0 mol %, $T$ = 165 ± 10 °C, and $t$ = 8 min. Similarly, the resulting extrudates were decross-linked and soluble in THF, reporting a negligible gel fraction.

Overall, it is demonstrated above that our catalytic PU decross-linking extrusion approach can be extended to decross-link aliphatic PU networks in an effective manner, expanding the library of feedstock cross-linked PUs for this approach.



https://doi.org/10.1021/jacsau.4c00403
JACS Au 2024, 4, 3058−3069

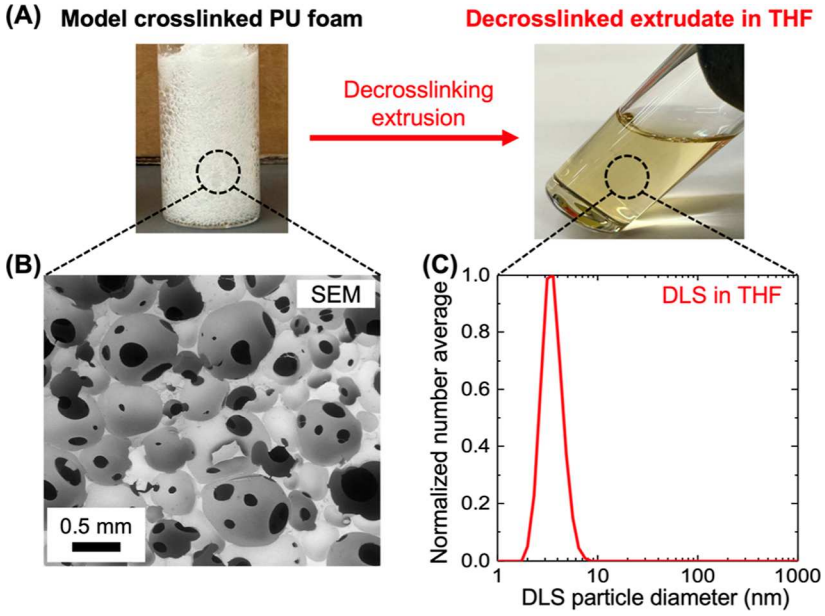


**Figure 3.** (A) Schematic diagram showing that model cross-linked PU foam undergoes small-molecule carbamate-assisted decross-linking extrusion to form decross-linked PU extrudate soluble in THF; (B) representative SEM image of the model cross-linked PU foam in (A); and (C) DLS spectrum of a dilute solution of the resulting **M1**-decross-linked extrudate in THF.

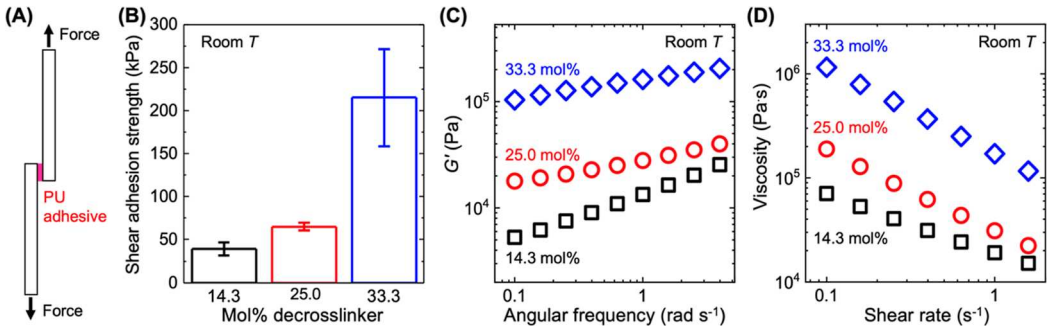


**Figure 4.** (A) Lap shear test assembly for measuring the shear adhesion strength of decross-linked PU extrudates; (B) room-temperature lap shear adhesion strength of the **M1**-decross-linked model PU film extrudates obtained at various decross-linker loadings; (C) room-temperature G′ vs frequency, and (D) room-temperature viscosity vs shear rate dependences for the decross-linked PU extrudates in (B). The error bars in (B) are standard deviations from five measurements.

**3.3.3. Extension to Model Cross-Linked PUFs.** We finally extended our approach to decross-link a model cross-linked PUF. PUFs are of interest because they comprise ∼70% of the entire PU market.[68] Herein, model cross-linked PUFs (Figure 3A) were synthesized by step-growth polymerization of a slightly off-stoichiometric mixture of the same triol and TDI, as shown in Section 3.2, (−OH/−NCO = 1:1.05) in the presence of catalytic amounts of DBTDL (0.5 mol % of the total −OH groups) and $H_2O$ (30 mol % of the total −OH groups) as a chemical blowing agent. In addition to the −OH/−NCO reactions between triol and TDI, $H_2O$ reacts with the isocyanate to form carbamic acid, which then decarboxylates to produce a primary amine while releasing gaseous $CO_2$ to trigger the subsequent foaming process.[3] These amines can further react with isocyanate groups to produce urea linkages in the synthesized model PU foam. According to SEM characterizations, the synthesized model PUFs show a semiopen cell geometry with an average cell diameter of 550 ± 130 $\mu$m (Figure 3B). In addition, swelling tests on this model PU foam confirm its cross-linking nature and report a relatively high gel fraction of ∼96 wt %, consistent with the nearly full functional group conversion measured by FTIR (Figure S22). This model cross-linked PU foam reports a $T_g$ of ∼−26 °C by DSC (Figure S22), slightly higher than that of the model cross-linked PU film. In addition, it reports a $T_d$ of ∼275 °C by TGA (Figure S22), nearly identical to that of the model cross-linked PU film.

Similarly, complete network deconstruction of this model cross-linked PU foam was achieved by reactive extrusion of the ground foams (average particle diameter of 1.4 ± 0.7 mm; measured by SEM; Figure S23) in the presence of 25.0 mol % **M1** under nearly identical reaction conditions, i.e., DBTDL loading = 4.0 mol %, $T$ = 165 ± 10 °C, and $t$ = 8 min. The resulting decross-linked extrudate is soluble in THF (Figure 3A), whose DLS spectrum reports a $D_h$ distribution with a peak centered at ∼3.6 nm (Figure 3C). Consistently, rheological frequency sweep experiments and FTIR/NMR analyses on the resulting extrudates confirm the complete network deconstruction of this model cross-linked PU foam after small-molecule carbamate-assisted decross-linking extrusion (Figure S24).


https://doi.org/10.1021/jacsau.4c00403
JACS Au 2024, 4, 3058−3069

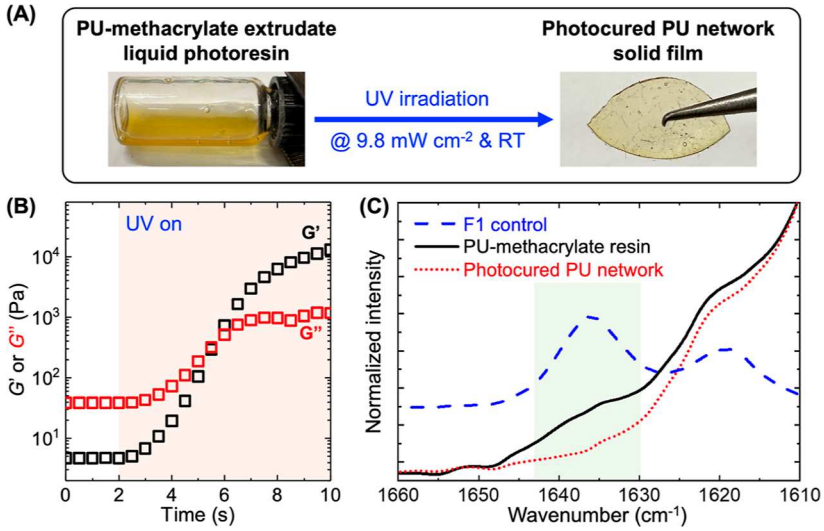


**Figure 5.** (A) Schematic diagram showing that the upcycled PU-methacrylate liquid photoresin undergoes UV curing at room temperature to form a cross-linked PU-methacrylate network solid film; (B) evolution of $G'$ and $G''$ of this PU-methacrylate photoresin during UV curing, where UV light is turned on 2 s into the rheological run and $G'$ and $G''$ cross over after ∼4 s of UV irradiation; and (C) FTIR spectra of this PU-methacrylate photoresin before and after UV curing, together with a **F1** control spectrum to demonstrate the disappearance of the methacrylate groups in the PU-methacrylate photoresin after UV curing.

Overall, these results demonstrate that our catalytic PU decross-linking extrusion approach can be extended from cross-linked PU films to PUFs that have additional porous structures and polyurea microdomains, without sacrificing the decross-linking efficiency of this dynamic carbamate exchange-based approach. This represents a promising route to recycle/upcycle postconsumer/waste cross-linked PUFs in a solvent-free and relatively high-throughput manner.

### 3.4. Structure–Property–Function Relationships in Decross-Linked and Functionalized PUs

Sections 3.2 and 3.3 have demonstrated that our platform small-molecule carbamate-assisted decross-linking extrusion approach can simultaneously deconstruct PU networks and functionalize the resulting decross-linked PU chains. This section highlights three potential applications of these decross-linked and functionalized PU products, i.e., adhesives, photoresins, and stimuli-responsive materials, with an emphasis on their structure–property–function relationships.

**3.4.1. Adhesives.** PUs offer good adhesion with a wide range of substrates, including metals, plastics, wood, glass, and ceramics, mainly due to the strong hydrogen bonding capabilities of the polar sites on their carbamate linkages.[69] For adhesive application demonstration, the **M1**-decross-linked PU film extrudates obtained at various decross-linker loadings, as shown in Section 3.2, were selected for adhesion tests. Specifically, these as-obtained model **M1**-decross-linked PU extrudates, without any additional purification/formulation, were directly sandwiched between two fresh microscope glass slides to form an assembly, as shown in Figure 4A (see geometry details in Figure S25). Their room-temperature overlap shear adhesion properties were tested by a tensile tester at a rate of 5 mm $min^{-1}$,[70,71] and the measured lap shear strength values are plotted in Figure 4B.

According to Figure 4B, the lap shear adhesion strength of **M1**-decross-linked PU film extrudates increases from ∼39 to ∼215 kPa as the **M1** loading increases from 14.3 to 33.3 mol %. We attribute this increase to a larger concentration of carbamate linkages capable of hydrogen bonding in the decross-linked PU extrudate obtained at a higher **M1** loading, thus enhancing its lap shear adhesion strength. One evidence for this is that these PU extrudates' $G'$ (Figure 4C) and viscosity (Figure 4D) at room temperature (where the hydrogen bonding between carbamate linkages is relatively strong) increase with increasing **M1** loading, although decross-linked PUs' molecular weight and thus melt viscosity at 80 °C decrease with increasing **M1** loading (Figure S12), as already discussed in Section 3.2.

Overall, these results demonstrate that the adhesion performance of these decross-linked PU extrudates can be systematically controlled by simply varying the loading of small-molecule carbamate decross-linkers. Future studies are warranted to further enhance the hydrogen bonding and thus the adhesion properties of these decross-linked PU extrudates to enable real-world adhesive applications, potentially through structural design of small-molecule carbamate decross-linkers.

**3.4.2. Photoresins.** As already established in Section 3.3.1, methacrylate groups can be covalently attached onto the decross-linked PU extrudates using our platform decross-linking extrusion approach, which can serve as reactive moieties for subsequent thermal or photochemical curing processes.[72,73] For photoresin application demonstration, the methacrylate-functionalized PU extrudates after dialysis were combined with 3 wt % radical photoinitiators, and the resulting mixture was cured at room temperature under ultraviolet (UV) light irradiation at an intensity of 9.8 mW $cm^{-2}$ (Figure 5A and Supporting Information). Promisingly, this PU-methacrylate photoresin exhibits relatively fast curing kinetics, reporting a crossover of $G'$ and $G''$ (also known as the gel point[74]) after ∼4 s of UV light irradiation (Figure 5B). After photocuring for 15 s at room temperature, the characteristic FTIR peak of the methacrylate group in the **F1**-decross-linked PU extrudate nearly disappeared due to methacrylate homopolymerization (Figure 5C). As a result, the liquid PU-methacrylate photoresin transforms into a cross-linked solid (Figure 5A), reporting a gel fraction of ∼90 wt %. In addition, these photocured samples report increased $T_g$ and $T_d$ values after methacrylate homopolymerization (Figure S26). Notably,


https://doi.org/10.1021/jacsau.4c00403
JACS Au 2024, 4, 3058–3069

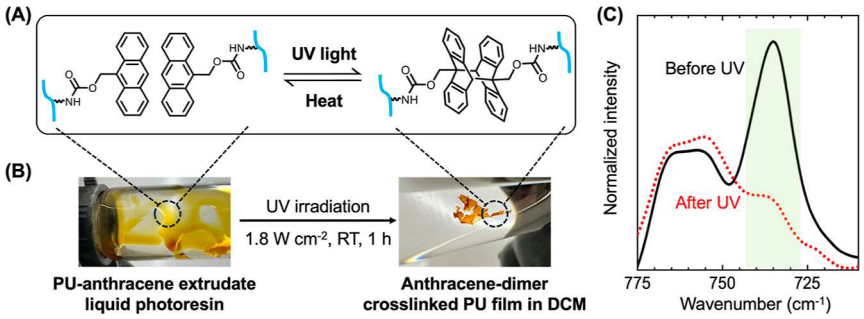


**Figure 6.** (A) Scheme showing that anthracene-functionalized chains can undergo dimerization under low-energy UV light irradiation to form anthracene-dimer linkages between chains, which are able to revert to free anthracene groups upon heating or high-energy UV light irradiation; (B) schematic diagram showing that liquid anthracene-functionalized PU extrudates transform into cross-linked PU films insoluble in dichloromethane (DCM); and (C) FTIR spectra of this PU-anthracene extrudate before and after UV irradiation, demonstrating anthracene dimerization.

these photocured PU-methacrylate networks comprise >90 wt % of PU segments and should be able to undergo stress relaxation or self-healing through dynamic topological rearrangement/reconfiguration among PU segments in the presence of carbamate exchange catalysts.[47]

Overall, these results demonstrate that our PU network decross-linking extrusion approach can produce reactive (meth)acrylate-functionalized PU thermoplastics that can hold promise for applications including coating, packaging, and 3D printing.[39,42−47] Currently, our group is optimizing these upcycled PU photoresins for vat polymerization-based 3D printing processes,[39,43−47] which can fabricate next-generation PUFs with well-controlled and programmable porous structures.

**3.4.3. Stimuli-Responsive Materials.** As already established in Section 3.3.1, our catalytic PU decross-linking extrusion approach can lead to PU chains functionalized with anthracene and stilbene groups, both of which are highly attractive in the field of stimuli-responsive materials.[75−80] For example, anthracene groups are known to undergo efficient [4 + 4]-cycloaddition under low-energy UV light ($\lambda$ > 300 nm) irradiation, forming anthracene-dimers that can reversibly cleave into free anthracenes, by either high-energy UV light ($\lambda$ < 300 nm) irradiation[81] or high-temperature annealing (Figure 6A).[80] For demonstration, the anthracene-functionalized PU extrudate after dialysis was irradiated with $\lambda$ > 300 nm UV light and an intensity of 1.8 W cm$^{-2}$ (Figure 6B). After photocuring for ∼1 h, the anthracene groups in the **F2**-decross-linked PU extrudate report a conversion of ∼90%, as measured by FTIR (Figure 6C). As a result of photodimerization, this anthracene-functionalized PU transitions from a liquid to an insoluble cross-linked solid (Figure 6B) reporting a gel fraction of ∼95 wt %. Similarly, the photocured sample reports an increased $T_g$ after anthracene dimerization (Figure S27). Importantly, the formed anthracene-dimer linkages can reversibly cleave and revert to free anthracene groups after heating above ∼200 °C.[77]

Overall, these results demonstrate that our platform decross-linking extrusion approach can enable the upcycling of cross-linked PU networks into functional thermoplastic PUs comprising various stimuli-responsive groups, which can be subsequently used for fabricating self-healing materials or dynamic CANs.[82,83]

## 4. CONCLUSIONS

In conclusion, this study reports a solvent-free and scalable decross-linking extrusion approach that can recycle/upcycle PU thermosets into low-viscosity, functional PU thermoplastics. This process exploits the use of small-molecule carbamate decross-linkers to simultaneously deconstruct cross-linked PUs and functionalize the decross-linked PU chains, through catalyzed carbamate exchange reactions in a twin-screw extruder. This small-molecule carbamate-assisted PU decross-linking extrusion approach offers several advantages: (1) it requires relatively mild reaction conditions, ensures fast reaction rates, and is compatible with the well-established polymer processing equipment; (2) it is versatile and generalizable to cross-linked PUs having various backbone chemistries (e.g., aromatic and aliphatic backbones) and form factors (e.g., films and foams) as well as small-molecule carbamate decross-linkers having various steric/electronic structures and chemical functionalities (e.g., methacrylate, anthracene, and stilbene groups); (3) it is highly modular, and one can systematically control the structure−property−function relationships in the resulting decross-linked PU extrudates by varying process parameters such as decross-linker loading; and (4) it is potentially capable of transforming postconsumer PU thermosets at scale into a library of low-viscosity and value-added thermoplastic PU feedstocks for diverse applications, including adhesives, photoresins, and stimuli-responsive materials. Therefore, we expect that this PU recycling/upcycling approach will help foster a more sustainable and circular PU ecosystem. We also expect that this decross-linking extrusion approach can serve as a platform to potentially transform many other step-growth networks (e.g., polyureas and polyesters) into a multitude of specialty polymers, thus providing alternative green chemistry solutions toward the growing economic/environmental concerns of plastic waste management.

## ■ ASSOCIATED CONTENT

### Supporting Information

The Supporting Information is available free of charge at https://pubs.acs.org/doi/10.1021/jacsau.4c00403.

Additional materials, syntheses, and instrumentation with full experimental and characterization details; results and discussion; and references (PDF)

## ■ AUTHOR INFORMATION

### Corresponding Authors

**Timothy E. Long** − *Chemical Engineering, School for Engineering of Matter, Transport and Energy, Arizona State University, Tempe 85287 Arizona, United States; Biodesign*



https://doi.org/10.1021/jacsau.4c00403
JACS Au 2024, 4, 3058−3069

*Center for Sustainable Macromolecular Materials and Manufacturing and Chemistry, School of Molecular Sciences, Arizona State University, Tempe 85287 Arizona, United States;* orcid.org/0000-0001-9515-5491;
Email: Timothy.E.Long@asu.edu

**Kailong Jin** − *Chemical Engineering, School for Engineering of Matter, Transport and Energy, Arizona State University, Tempe 85287 Arizona, United States; Biodesign Center for Sustainable Macromolecular Materials and Manufacturing, Arizona State University, Tempe 85287 Arizona, United States;* orcid.org/0000-0001-5428-3227;
Email: Kailong.Jin@asu.edu

## Authors

**Jared A. Nettles** − *Chemical Engineering, School for Engineering of Matter, Transport and Energy, Arizona State University, Tempe 85287 Arizona, United States; Biodesign Center for Sustainable Macromolecular Materials and Manufacturing, Arizona State University, Tempe 85287 Arizona, United States*

**Saleh Alfarhan** − *Chemical Engineering, School for Engineering of Matter, Transport and Energy, Arizona State University, Tempe 85287 Arizona, United States; Biodesign Center for Sustainable Macromolecular Materials and Manufacturing, Arizona State University, Tempe 85287 Arizona, United States;* orcid.org/0009-0005-2629-5948

**Cameron A. Pascoe** − *Biodesign Center for Sustainable Macromolecular Materials and Manufacturing, Arizona State University, Tempe 85287 Arizona, United States*

**Clarissa Westover** − *Biodesign Center for Sustainable Macromolecular Materials and Manufacturing and Materials Science and Engineering, School for Engineering of Matter, Transport and Energy, Arizona State University, Tempe 85287 Arizona, United States;* orcid.org/0000-0002-8095-3412

**Margaret D. Madsen** − *Biodesign Center for Sustainable Macromolecular Materials and Manufacturing and Chemistry, School of Molecular Sciences, Arizona State University, Tempe 85287 Arizona, United States;* orcid.org/0009-0000-8481-7621

**Jose I. Sintas** − *Biodesign Center for Sustainable Macromolecular Materials and Manufacturing and Chemistry, School of Molecular Sciences, Arizona State University, Tempe 85287 Arizona, United States;* orcid.org/0000-0001-7789-2578

**Aadhi Subbiah** − *Department of Chemical and Biological Engineering, Iowa State University, Ames 50011 Iowa, United States*

Complete contact information is available at: https://pubs.acs.org/10.1021/jacsau.4c00403

## Author Contributions

**Jared Nettles**: conceptualization, methodology, validation, writing—original draft, writing—review and editing; **Saleh Alfarhan**: methodology; writing—review and editing; **Cameron A. Pascoe**: methodology; writing—review and editing; **Clarissa Westover**: methodology; writing—review and editing; **Margaret D. Madsen**: methodology, writing—review and editing; **Jose I. Sintas**: methodology, writing—review and editing; **Aadhi Subbiah**: methodology; writing—review and editing; **Timothy E. Long**: funding acquisition, supervision, writing—review and editing; **Kailong Jin**: conceptualization, funding acquisition, validation, supervision, project administration, writing—review and editing. All authors have given approval to the final version of the manuscript.

## Notes

The authors declare no competing financial interest.

## ■ ACKNOWLEDGMENTS

This study is based upon work supported by the National Science Foundation under grant no. 2132183. K.J. also acknowledges the startup research funding support provided by the Ira A. Fulton Schools of Engineering at Arizona State University (ASU) and from the National Institute of Standards and Technology (NIST-60NANB22D138). The authors acknowledge Morgan Nunez (an undergraduate REM student) for contributing to the installation of the twin-screw extruder used in this study and Rose McDonough (a graduate student in the Long group) for performing size exclusion chromatography analysis during the manuscript revision process. Finally, the authors acknowledge the Biodesign Center for Sustainable Macromolecular Materials and Manufacturing at ASU for the access and use of shared facilities.

## ■ REFERENCES

(1) Insights, F. B. *Polyurethane Market Size, Share & Industry Analysis, By Product Type (Rigid Foam, Flexible Foam, Molded Foam, Elastomers, Adhesives & Sealants, Coatings, and Others), By Application (Furniture, Construction, Electronics, Automotive, Packaging, Footwear, and Others), and Regional Forecast, 2024−2032*. Report ID: FBI101801; Fortune Business Insights, 2024. https://www.fortunebusinessinsights.com/industry-reports/polyurethane-pu-market-101801.

(2) Statista Research Department. *Market Volume of Polyurethane Worldwide from 2015 to 2022, with a Forecast for 2023 to 2030*; AgileIntel Research (ChemIntel360), 2023. https://www.statista.com/statistics/720341/global-polyurethane-market-size-forecast/.

(3) Frisch, K. C.; Klempner, D. 24—Polyurethanes. In *Comprehensive Polymer Science and Supplements*; Allen, G., Bevington, J. C., Eds.; Pergamon: Amsterdam, 1989; pp 413−426.

(4) Akindoyo, J. O.; Beg, M. D. H.; Ghazali, S.; Islam, M. R.; Jeyaratnam, N.; Yuvaraj, A. R. Polyurethane types, synthesis and applications-a review. *RSC Adv.* **2016**, *6* (115), 114453−114482.

(5) Das, A.; Mahanwar, P. A brief discussion on advances in polyurethane applications. *Adv. Ind. Eng. Polym. Res.* **2020**, *3* (3), 93−101.

(6) Delavarde, A.; Savin, G.; Derkenne, P.; Boursier, M.; Morales-Cerrada, R.; Nottelet, B.; Pinaud, J.; Caillol, S. Sustainable polyurethanes: toward new cutting-edge opportunities. *Prog. Polym. Sci.* **2024**, *151*, 101805.

(7) Liang, C.; Gracida-Alvarez, U. R.; Gallant, E. T.; Gillis, P. A.; Marques, Y. A.; Abramo, G. P.; Hawkins, T. R.; Dunn, J. B. Material Flows of Polyurethane in the United States. *Environ. Sci. Technol.* **2021**, *55* (20), 14215−14224.

(8) Self, J. L.; Zervoudakis, A. J.; Peng, X.; Lenart, W. R.; Macosko, C. W.; Ellison, C. J. Linear, Graft, and Beyond: Multiblock Copolymers as Next-Generation Compatibilizers. *JACS Au* **2022**, *2* (2), 310−321.

(9) Banik, J.; Chakraborty, D.; Rizwan, M.; Shaik, A. H.; Chandan, M. R. Review on disposal, recycling and management of waste polyurethane foams: A way ahead. *Waste Manage. Res.* **2023**, *41* (6), 1063−1080.

(10) Simioni, F.; Bisello, S.; Tavan, M. Polyol recovery from rigid polyurethane waste. *Cell. Polym.* **1983**, *2* (4), 281−293.

(11) Chuayjuljit, S.; Norakankorn, C.; Pimpan, V. Chemical recycling of rigid polyurethane foam scrap via base catalyzed aminolysis. *J. Met., Mater. Miner.* **2002**, *12* (1), 19−22.

(12) Gama, N.; Godinho, B.; Marques, G.; Silva, R.; Barros-Timmons, A.; Ferreira, A. Recycling of polyurethane scraps via acidolysis. *Chem. Eng. J.* **2020**, *395*, 125102.
(13) Campbell, G. A.; Meluch, W. C. Polyurethane foam recycling. Superheated steam hydrolysis. *Environ. Sci. Technol.* **1976**, *10* (2), 182−185.
(14) Magnin, A.; Pollet, E.; Avérous, L. Chapter Fifteen—Characterization of the enzymatic degradation of polyurethanes. In *Methods in Enzymology*; Weber, G., Bornscheuer, U. T., Wei, R., Eds.; Academic Press, 2021; Vol. *648*, pp 317−336.
(15) Simón, D.; Borreguero, A.; De Lucas, A.; Rodríguez, J. Recycling of polyurethanes from laboratory to industry, a journey towards the sustainability. *Waste Manage.* **2018**, *76*, 147−171.
(16) Garcia, J. M.; Robertson, M. L. The future of plastics recycling. *Science* **2017**, *358* (6365), 870−872.
(17) Kloxin, C. J.; Scott, T. F.; Adzima, B. J.; Bowman, C. N. Covalent Adaptable Networks (CANs): A Unique Paradigm in Cross-Linked Polymers. *Macromolecules* **2010**, *43* (6), 2643−2653.
(18) Miravalle, E.; Bracco, P.; Brunella, V.; Barolo, C.; Zanetti, M. Improving Sustainability through Covalent Adaptable Networks in the Recycling of Polyurethane Plastics. *Polymers* **2023**, *15* (18), 3780.
(19) Fortman, D. J.; Sheppard, D. T.; Dichtel, W. R. Reprocessing Cross-Linked Polyurethanes by Catalyzing Carbamate Exchange. *Macromolecules* **2019**, *52* (16), 6330−6335.
(20) Brutman, J. P.; Fortman, D. J.; De Hoe, G. X.; Dichtel, W. R.; Hillmyer, M. A. Mechanistic study of stress relaxation in urethane-containing polymer networks. *J. Phys. Chem. B* **2019**, *123* (6), 1432−1441.
(21) Sheppard, D. T.; Jin, K.; Hamachi, L. S.; Dean, W.; Fortman, D. J.; Ellison, C. J.; Dichtel, W. R. Reprocessing Postconsumer Polyurethane Foam Using Carbamate Exchange Catalysis and Twin-Screw Extrusion. *ACS Cent. Sci.* **2020**, *6* (6), 921−927.
(22) Kim, S.; Li, K.; Alsbaiee, A.; Brutman, J. P.; Dichtel, W. R. Circular Reprocessing of Thermoset Polyurethane Foams. *Adv. Mater.* **2023**, *35* (41), 2305387.
(23) Zheng, N.; Fang, Z.; Zou, W.; Zhao, Q.; Xie, T. Thermoset shape-memory polyurethane with intrinsic plasticity enabled by transcarbamoylation. *Angew. Chem.* **2016**, *128* (38), 11593−11597.
(24) Wen, Z.; McBride, M. K.; Zhang, X.; Han, X.; Martinez, A. M.; Shao, R.; Zhu, C.; Visvanathan, R.; Clark, N. A.; Wang, Y.; et al. Reconfigurable LC elastomers: Using a thermally programmable monodomain to access two-way free-standing multiple shape memory polymers. *Macromolecules* **2018**, *51* (15), 5812−5819.
(25) Chen, X.; Hu, S.; Li, L.; Torkelson, J. M. Dynamic Covalent Polyurethane Networks with Excellent Property and Cross-Link Density Recovery after Recycling and Potential for Monomer Recovery. *ACS Appl. Polym. Mater.* **2020**, *2* (5), 2093−2101.
(26) Yan, P.; Zhao, W.; Fu, X.; Liu, Z.; Kong, W.; Zhou, C.; Lei, J. Multifunctional polyurethane-vitrimers completely based on trans-carbamoylation of carbamates: thermally-induced dual-shape memory effect and self-welding. *RSC Adv.* **2017**, *7* (43), 26858−26866.
(27) Aguirresarobe, R. H.; Nevejans, S.; Reck, B.; Irusta, L.; Sardon, H.; Asua, J. M.; Ballard, N. Healable and self-healing polyurethanes using dynamic chemistry. *Prog. Polym. Sci.* **2021**, *114*, 101362.
(28) Montarnal, D.; Capelot, M.; Tournilhac, F.; Leibler, L. Silica-like malleable materials from permanent organic networks. *Science* **2011**, *334* (6058), 965−968.
(29) Röttger, M.; Domenech, T.; van Der Weegen, R.; Breuillac, A.; Nicolaÿ, R.; Leibler, L. High-performance vitrimers from commodity thermoplastics through dioxaborolane metathesis. *Science* **2017**, *356* (6333), 62−65.
(30) Scott, T. F.; Schneider, A. D.; Cook, W. D.; Bowman, C. N. Photoinduced Plasticity in Cross-Linked Polymers. *Science* **2005**, *308* (5728), 1615−1617.
(31) Elling, B. R.; Dichtel, W. R. Reprocessable cross-linked polymer networks: are associative exchange mechanisms desirable? *ACS Cent. Sci.* **2020**, *6* (9), 1488−1496.
(32) Denissen, W.; Winne, J. M.; Du Prez, F. E. Vitrimers: permanent organic networks with glass-like fluidity. *Chem. Sci.* **2016**, *7* (1), 30−38.
(33) Denissen, W.; Rivero, G.; Nicolaÿ, R.; Leibler, L.; Winne, J. M.; Du Prez, F. E. Vinylogous Urethane Vitrimers. *Adv. Funct. Mater.* **2015**, *25* (16), 2451−2457.
(34) Wojtecki, R. J.; Meador, M. A.; Rowan, S. J. Using the dynamic bond to access macroscopically responsive structurally dynamic polymers. *Nat. Mater.* **2011**, *10* (1), 14−27.
(35) Cash, J. J.; Kubo, T.; Bapat, A. P.; Sumerlin, B. S. Room-Temperature Self-Healing Polymers Based on Dynamic-Covalent Boronic Esters. *Macromolecules* **2015**, *48* (7), 2098−2106.
(36) Self, J. L.; Dolinski, N. D.; Zayas, M. S.; Read de Alaniz, J.; Bates, C. M. Brønsted-Acid-Catalyzed Exchange in Polyester Dynamic Covalent Networks. *ACS Macro Lett.* **2018**, *7* (7), 817−821.
(37) Ma, J.; Porath, L. E.; Haque, M. F.; Sett, S.; Rabbi, K. F.; Nam, S.; Miljkovic, N.; Evans, C. M. Ultra-thin self-healing vitrimer coatings for durable hydrophobicity. *Nat. Commun.* **2021**, *12* (1), 5210.
(38) Porath, L.; Soman, B.; Jing, B. B.; Evans, C. M. Vitrimers: Using Dynamic Associative Bonds to Control Viscoelasticity, Assembly, and Functionality in Polymer Networks. *ACS Macro Lett.* **2022**, *11* (4), 475−483.
(39) Robinson, L. L.; Self, J. L.; Fusi, A. D.; Bates, M. W.; Read de Alaniz, J.; Hawker, C. J.; Bates, C. M.; Sample, C. S. Chemical and Mechanical Tunability of 3D-Printed Dynamic Covalent Networks Based on Boronate Esters. *ACS Macro Lett.* **2021**, *10* (7), 857−863.
(40) Neidhart, E. K.; Hua, M.; Peng, Z.; Kearney, L. T.; Bhat, V.; Vashahi, F.; Alexanian, E. J.; Sheiko, S. S.; Wang, C.; Helms, B. A.; Leibfarth, F. A. C−H Functionalization of Polyolefins to Access Reprocessable Polyolefin Thermosets. *J. Am. Chem. Soc.* **2023**, *145* (50), 27450−27458.
(41) Zhang, Q.; Qu, D.-H.; Feringa, B. L.; Tian, H. Disulfide-Mediated Reversible Polymerization toward Intrinsically Dynamic Smart Materials. *J. Am. Chem. Soc.* **2022**, *144* (5), 2022−2033.
(42) Somarathna, H. M. C. C.; Raman, S. N.; Mohotti, D.; Mutalib, A. A.; Badri, K. H. The use of polyurethane for structural and infrastructural engineering applications: A state-of-the-art review. *Constr. Build. Mater.* **2018**, *190*, 995−1014.
(43) Tumbleston, J. R.; Shirvanyants, D.; Ermoshkin, N.; Janusziewicz, R.; Johnson, A. R.; Kelly, D.; Chen, K.; Pinschmidt, R.; Rolland, J. P.; Ermoshkin, A.; Samulski, E. T.; DeSimone, J. M. Continuous liquid interface production of 3D objects. *Science* **2015**, *347* (6228), 1349−1352.
(44) Chyr, G.; DeSimone, J. M. Review of high-performance sustainable polymers in additive manufacturing. *Green Chem.* **2023**, *25* (2), 453−466.
(45) Liu, Z.; Fang, Z.; Zheng, N.; Yang, K.; Sun, Z.; Li, S.; Li, W.; Wu, J.; Xie, T. Chemical upcycling of commodity thermoset polyurethane foams towards high-performance 3D photo-printing resins. *Nat. Chem.* **2023**, *15* (12), 1773−1779.
(46) Lopez de Pariza, X.; Varela, O.; Catt, S. O.; Long, T. E.; Blasco, E.; Sardon, H. Recyclable photoresins for light-mediated additive manufacturing towards Loop 3D printing. *Nat. Commun.* **2023**, *14* (1), 5504.
(47) Hamachi, L. S.; Rau, D. A.; Arrington, C. B.; Sheppard, D. T.; Fortman, D. J.; Long, T. E.; Williams, C. B.; Dichtel, W. R. Dissociative Carbamate Exchange Anneals 3D Printed Acrylates. *ACS Appl. Mater. Interfaces* **2021**, *13* (32), 38680−38687.
(48) Delebecq, E.; Pascault, J.-P.; Boutevin, B.; Ganachaud, F. On the Versatility of Urethane/Urea Bonds: Reversibility, Blocked Isocyanate, and Non-isocyanate Polyurethane. *Chem. Rev.* **2013**, *113* (1), 80−118.
(49) Sintas, J. I.; Wolfgang, J. D.; Long, T. E. Carbamate thermal decarboxylation for the design of non-isocyanate polyurethane foams. *Polym. Chem.* **2023**, *14* (13), 1497−1506.
(50) Król, P.; Uram, Ł.; Król, B.; Pielichowska, K.; Walczak, M. Study of chemical, physico-mechanical and biological properties of 4,4′-methylenebis(cyclohexyl isocyanate)-based polyurethane films. *Mater. Sci. Eng. C* **2018**, *93*, 483−494.


https://doi.org/10.1021/jacsau.4c00403
*JACS Au* 2024, 4, 3058−3069

(51) Hiemenz, P. C.; Lodge, T. P. *Polymer Chemistry* (2nd ed.), CRC Press: Taylor & Francis, 2007, 381−418.
(52) Sun, M.; Sheppard, D. T.; Brutman, J. P.; Alsbaiee, A.; Dichtel, W. R. Green Catalysts for Reprocessing Thermoset Polyurethanes. *Macromolecules* **2023**, *56* (17), 6978−6987.
(53) Dobrzynski, P.; Kasperczyk, J.; Janeczek, H.; Bero, M. Synthesis of biodegradable copolymers with the use of low toxic zirconium compounds. 1. Copolymerization of glycolide with L-lactide initiated by Zr (Acac) 4. *Macromolecules* **2001**, *34* (15), 5090−5098.
(54) Flory, P. J. Molecular size distribution in three dimensional polymers. I. Gelation1. *J. Am. Chem. Soc.* **1941**, *63* (11), 3083−3090.
(55) Stockmayer, W. H. Theory of molecular size distribution and gel formation in branched-chain polymers. *J. Chem. Phys.* **1943**, *11* (2), 45−55.
(56) Li, L.; Chen, X.; Jin, K.; Torkelson, J. M. Vitrimers Designed Both To Strongly Suppress Creep and To Recover Original Cross-Link Density after Reprocessing: Quantitative Theory and Experiments. *Macromolecules* **2018**, *51* (15), 5537−5546.
(57) Yildirim, E.; Yurtsever, M.; Yilgör, E.; Yilgör, I.; Wilkes, G. L. Temperature-dependent changes in the hydrogen bonded hard segment network and microphase morphology in a model polyurethane: Experimental and simulation studies. *J. Polym. Sci., Part B: Polym. Phys.* **2018**, *56* (2), 182−192.
(58) Saha, J. K.; Rahman, M. M.; Haq, M. B.; Al Shehri, D. A.; Jang, J. Theoretical and Experimental Studies of Hydrogen Bonded Dihydroxybenzene Isomers Polyurethane Adhesive Material. *Polymers (Basel)* **2022**, *14* (9), 1701.
(59) Zagar, E. Solution properties of polyurethanes studied by static light scattering, SEC-MALS, and viscometry. *Acta Chim. Slov.* **2005**, *52* (3), 245.
(60) Sato, H. Properties of dilute solutions of polyurethanes. II. Branched polymers. *Bull. Chem. Soc. Jpn.* **1966**, *39* (11), 2340−2344.
(61) Kamide, K.; Kiguchi, A.; Miyazaki, Y. Viscometric and light scattering study in dimethylacetamide of linear segment polyurethane, polymerized with methylene bis (4-phenyl isocyanate) polytetramethylene glycol and ethylene diamine. *Polym. J.* **1986**, *18* (12), 919−925.
(62) Sato, H. Properties of dilute solutions of polyurethanes. I. Linear polymers. *Bull. Chem. Soc. Jpn.* **1966**, *39* (11), 2335−2340.
(63) De Gennes, P. Dynamics of entangled polymer solutions. I. The Rouse model. *Macromolecules* **1976**, *9* (4), 587−593.
(64) Fujisawa, S.; Kadoma, Y.; Yokoe, I. Radical-scavenging activity of butylated hydroxytoluene (BHT) and its metabolites. *Chem. Phys. Lipids* **2004**, *130* (2), 189−195.
(65) Trovati, G.; Sanches, E. A.; Neto, S. C.; Mascarenhas, Y. P.; Chierice, G. O. Characterization of polyurethane resins by FTIR, TGA, and XRD. *J. Appl. Polym. Sci.* **2010**, *115* (1), 263−268.
(66) Rosu, D.; Rosu, L.; Cascaval, C. N. IR-change and yellowing of polyurethane as a result of UV irradiation. *Polym. Degrad. Stab.* **2009**, *94* (4), 591−596.
(67) Irusta, L.; Fernandez-Berridi, M. Photooxidative behaviour of segmented aliphatic polyurethanes. *Polym. Degrad. Stab.* **1999**, *63* (1), 113−119.
(68) Kemona, A.; Piotrowska, M. Polyurethane Recycling and Disposal: Methods and Prospects. *Polymers* **2020**, *12* (8), 1752.
(69) Segura, D. M.; Nurse, A. D.; McCourt, A.; Phelps, R.; Segura, A. Chapter 3 Chemistry of polyurethane adhesives and sealants. In *Handbook of Adhesives and Sealants*; Cognard, P., Ed.; Elsevier Science Ltd, 2005; Vol. *1*, pp 101−162.
(70) Wang, Y.; Yang, X.; Nian, G.; Suo, Z. Strength and toughness of adhesion of soft materials measured in lap shear. *J. Mech. Phys. Solids* **2020**, *143*, 103988.
(71) Kim, H. J.; Jin, K.; Shim, J.; Dean, W.; Hillmyer, M. A.; Ellison, C. J. Sustainable Triblock Copolymers as Tunable and Degradable Pressure Sensitive Adhesives. *ACS Sustainable Chem. Eng.* **2020**, *8* (32), 12036−12044.
(72) Beuermann, S.; Buback, M.; Davis, T. P.; Gilbert, R. G.; Hutchinson, R. A.; Olaj, O. F.; Russell, G. T.; Schweer, J.; Van Herk, A. M. Critically evaluated rate coefficients for free-radical polymerization, 2: Propagation rate coefficients for methyl methacrylate. *Macromol. Chem. Phys.* **1997**, *198* (5), 1545−1560.
(73) Sideridou, I.; Tserki, V.; Papanastasiou, G. Effect of chemical structure on degree of conversion in light-cured dimethacrylate-based dental resins. *Biomaterials* **2002**, *23* (8), 1819−1829.
(74) Chambon, F.; Winter, H. H. Stopping of crosslinking reaction in a PDMS polymer at the gel point. *Polym. Bull.* **1985**, *13*, 499−503.
(75) Roy, D.; Cambre, J. N.; Sumerlin, B. S. Future perspectives and recent advances in stimuli-responsive materials. *Prog. Polym. Sci.* **2010**, *35* (1−2), 278−301.
(76) Yokoe, M.; Yamauchi, K.; Long, T. E. Controlled radical polymerization of anthracene-containing methacrylate copolymers for stimuli-responsive materials. *J. Polym. Sci., Part A: Polym. Chem.* **2016**, *54* (15), 2302−2311.
(77) Jin, K.; Banerji, A.; Kitto, D.; Bates, F. S.; Ellison, C. J. Mechanically Robust and Recyclable Cross-Linked Fibers from Melt Blown Anthracene-Functionalized Commodity Polymers. *ACS Appl. Mater. Interfaces* **2019**, *11* (13), 12863−12870.
(78) Liu, X.; Xu, J.-F.; Wang, Z.; Zhang, X. Photo-responsive supramolecular polymers synthesized by olefin metathesis polymerization from supramonomers. *Polym. Chem.* **2016**, *7* (13), 2333−2336.
(79) Sun, H.; Kabb, C. P.; Sumerlin, B. S. Thermally-labile segmented hyperbranched copolymers: using reversible-covalent chemistry to investigate the mechanism of self-condensing vinyl copolymerization. *Chem. Sci.* **2014**, *5* (12), 4646−4655.
(80) Van Damme, J.; van den Berg, O.; Brancart, J.; Vlaminck, L.; Huyck, C.; Van Assche, G.; Van Mele, B.; Du Prez, F. Anthracene-Based Thiol−Ene Networks with Thermo-Degradable and Photo-Reversible Properties. *Macromolecules* **2017**, *50* (5), 1930−1938.
(81) Chandross, E. A. Photolytic dissociation of dianthracene. *J. Chem. Phys.* **1965**, *43* (11), 4175−4176.
(82) Fang, Y.; Du, X.; Du, Z.; Wang, H.; Cheng, X. Light- and heat-triggered polyurethane based on dihydroxyl anthracene derivatives for self-healing applications. *J. Mater. Chem. A* **2017**, *5* (17), 8010−8017.
(83) Van Damme, J.; Du Prez, F. Anthracene-containing polymers toward high-end applications. *Prog. Polym. Sci.* **2018**, *82*, 92−119.


https://doi.org/10.1021/jacsau.4c00403
*JACS Au* 2024, 4, 3058−3069